Electronic Supplementary Material (ESI) for Chemical Communications.

# Supporting information for

# A Ferrocene Based Switchable Molecular Folding Ruler

Synøve Ø. Scottwell,[a] Jonathan E. Barnsley,[a,b] C. John McAdam,[a] Keith C. Gordon,[a,b] and James D. Crowley[a]*

[a] Department of Chemistry, University of Otago, PO Box 56, Dunedin, New Zealand.

[b] MacDiarmid Institute for Advanced Materials and Nanotechnology, New Zealand

*E-mail: jcrowley@chemistry.otago.ac.nz, Fax: +64 3 479 7906; Tel: +64 3 479 7731.

# Contents

# 1 General experimental

Unless otherwise stated, all reagents were purchased from commercial sources and used without further purification. The precursor 1-(5-yl-ethynyl-2,2′-bipyridine)-1′-iodo-ferrocene and ligand 6,6′-dimesityl-2,2′-bipyridine were synthesised according to previously reported procedures.[1] Solvents were laboratory reagent grade, with the following exceptions: dry tetrahydrofuran (THF) and dichloromethane ($CH_2Cl_2$) were obtained by passing the solvents through an activated alumina column on a PureSolv TM solvent purification system (Innovative Technologies, Inc., Amesbury, MA, USA). Petroleum ether (petrol) refers to the fraction of petrol boiling in the range 40-60 °C, ethylenediaminetetraacetate (EDTA), and dimethylformamide (DMF). $^{1}H$ and $^{13}C$ NMR spectra were recorded on either a 400 MHz Varian/Agilent 400 MR or Varian/Agilent 500 MHz AR spectrometer at 298 K. Chemical shifts are reported in parts per million (ppm) and referenced to residual solvent peaks ($CDCl_3$: $^{1}H$ $\delta$ 7.26, $^{13}C$ $\delta$ 77.16 ppm). Coupling constants (J) are reported in Hertz (Hz). Standard abbreviations indicating multiplicity were used as follows: s = singlet, d = doublet, t = triplet, qt = quartet, m = multiplet, and dd = double doublet. IR spectra were recorded on a Bruker optics ALPHA FT-IR spectrometer equipped with a diamond ATR accessory. Elemental analyses were performed at the Campbell Microanalytical Laboratory, University of Otago. High resolution electrospray ionization mass spectra (HR-ESI-MS) were collected on a Bruker micrOTOF-Q spectrometer. UV-Visible absorption spectra were acquired with a Shimadzu UV-2600 spectrophotometer in acetonitrile ($10^{-5}$ M concentrations).

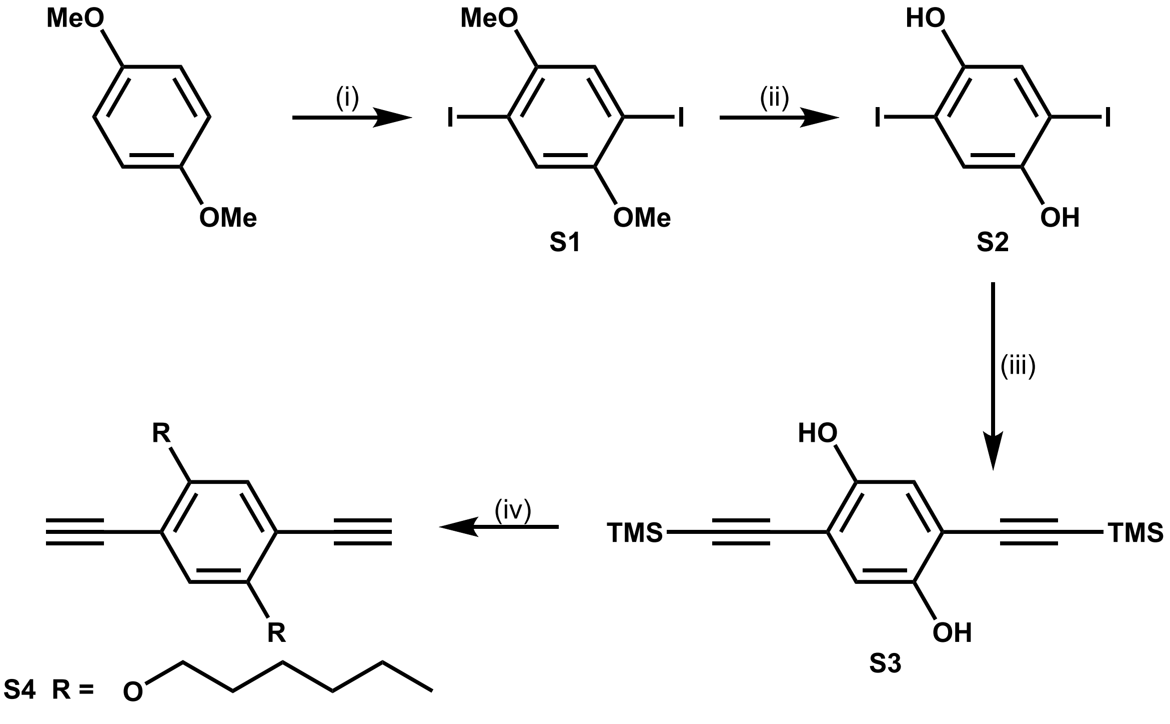

**Scheme S1** (i) $I_2$ (1.2 eq.), $KIO_3$ (1.2 eq.), 90:7:3 glacial acetic acid/$H_2O$/$H_2SO_4$, 70 °C (24 h); (ii) $BBr_3$ (4.25 eq.), $CH_2Cl_2$, -78 °C (10 min) then 25 °C (16 h); (iii) ethynyltrimethylsilane (2.5 eq.), $[PdCl_2(PPh_3)_2]$ (0.03 eq.), CuI (0.1 eq.), triethylamine (6 eq.), THF, reflux (24 h); (iv) 1-bromohexane (2.2 eq.), $K_2CO_3$ (3 eq.), DMF, 50 °C (16 h).

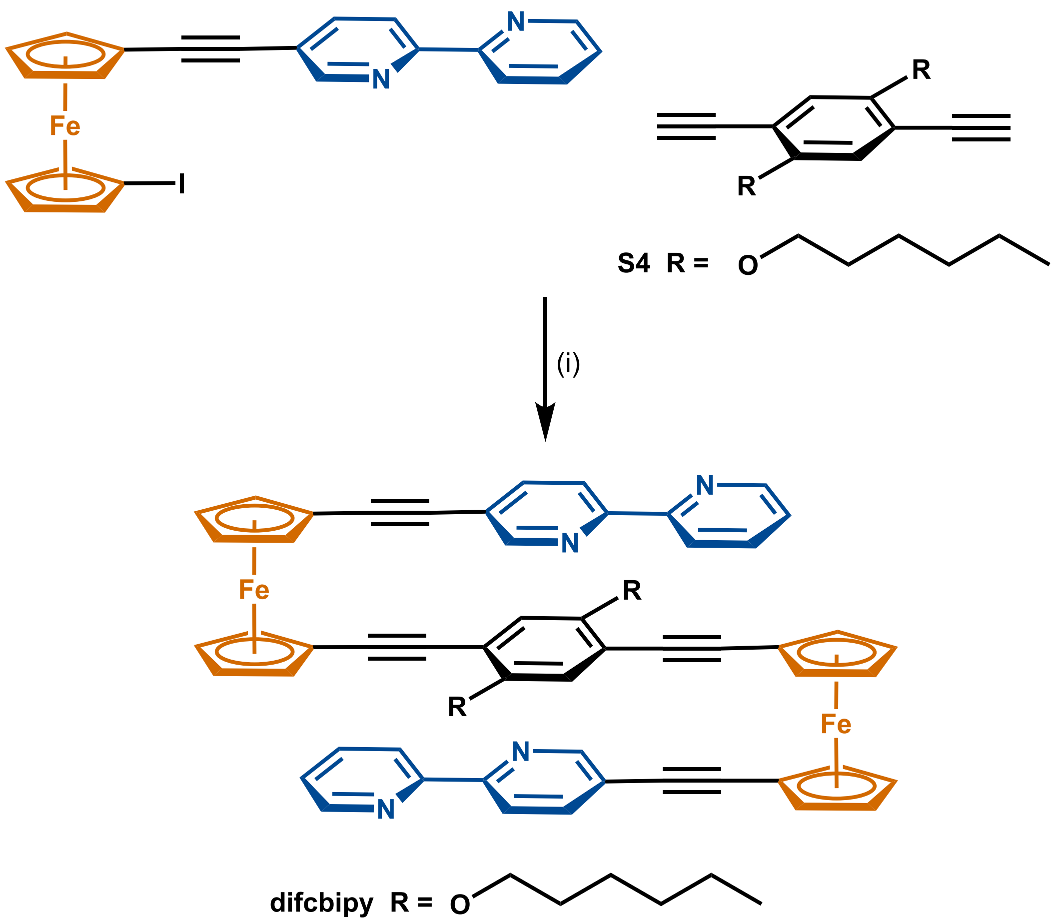

**Scheme S2** (i) [$Pd(CH_3CN)_2Cl_2$] (0.06 eq.), [$PH(^tBu)_3$]$BF_4$ (0.12 eq.), CuI (0.2 eq.), diisopropylamine, 300 W, 100 °C (2 h).

## 1.1 1,4-Diiodo-2,5-dimethoxybenzene (S1)

This compound was synthesised using an adapted methodology by Shinkai *et al.* who synthesised it previously in 58% yield.[2]

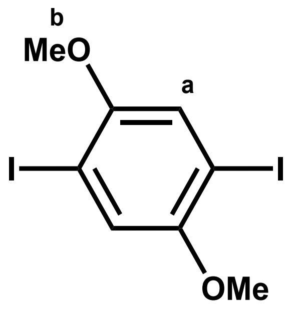

Iodine (33.1 g, 130 mmol, 1.20 eq.), potassium iodate (27.9 g, 130 mmol, 1.20 eq.), and 1,4-dimethoxybenzene (15.0 g, 109 mmol, 1.00 eq.) were combined in 90:7:3 glacial acetic acid/water/concentrated $H_2SO_4$ (100 mL) under a nitrogen atmosphere. The solution was heated at 70 °C for 24 hours, then allowed to cool to room temperature and poured into water (500 mL). The crude solid was collected by vacuum filtration, then recrystallised from THF/water to give the pure product as a cream solid. Yield: 29.8 g, 71%. Mp 173 ˚C; $^1H$ NMR (400 MHz, $CDCl_3$) δ 7.19 (s, 2H, $H_a$), 3.82 (s, 6H, $H_b$); $^{13}C$ NMR (125 MHz, $CDCl_3$) δ 153.5, 121.7, 85.6, 57.3; IR (ATR): ν (cm$^{-1}$) 2830, 1682, 1481, 1346, 1271, 1201, 1057, 1014, 837, 743, 432; HRESI-MS (CH$_3$OH) *m/z* = 412.8607 [**S1**+Na]$^+$ (calc. for $C_8H_8I_2O_2Na$ 412.8506), *m/z* = 428.8055 [**S1**+K]$^+$ (calc. for $C_8H_8I_2O_2K$ 428.8245); Anal. Calc. for $C_8H_8I_2O_2$: C, 24.64; H, 2.07; N, 0.00%. Found: C, 24.87; H, 2.01; N, 0.00%.

### 1.2 2,5-Diiodo-1,4-benzenediol (S2)

This compound was synthesised using an adapted methodology by Thomas *et al.* who synthesised it previously in 71% yield.[3]

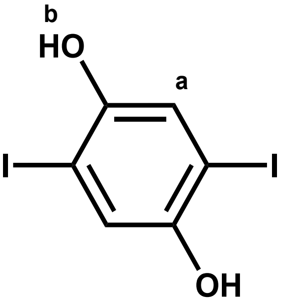

Dry CH$_2$Cl$_2$ (150 mL) was added to **S1** (5.00 g, 12.8 mmol, 1.00 eq.) under argon and cooled to -78 °C. After stirring for ten minutes, BBr$_3$ (13.65 g, 54.5 mmol, 4.25 eq.) was carefully added. The solution was allowed to warm to room temperature, stirred overnight (16 hours), then poured into ice water (500 mL). The white precipitated product was collected via vacuum filtration. Yield: 4.56 g, 98%. Mp 200 °C; $^1$H NMR (400 MHz, CDCl$_3$) δ 7.29 (s, 2H, H$_a$), 5.12 (s, 2H, H$_b$); $^{13}$C NMR (125 MHz, CDCl$_3$) δ 149.7, 123.2, 86.0; IR (ATR): ν (cm$^{-1}$) 3427, 3134, 1636, 1389, 1188, 1048, 871, 852, 789, 643, 569, 444, 426; HRESI-MS (CH$_3$OH) *m/z* = 360.8227 [**S2**-H]$^-$ (calc. for $C_6H_3I_2O_2$ 360.8228); Anal. Calc. for $C_8H_8I_2O_2$: C, 19.91; H, 1.11; N, 0.00%. Found: C, 19.96; H, 1.12; N, 0.00%.

### 1.3 2,5-Bis(2-(trimethylsilyl)ethynyl)-1,4-benzenediol (S3)

This compound has previously been synthesised by Johnson *et al.* through an alternative methodology from the bis(1,1-difluoro-2,2-dichloroethyl)ether of hydroquinone in 70% yield.[4]

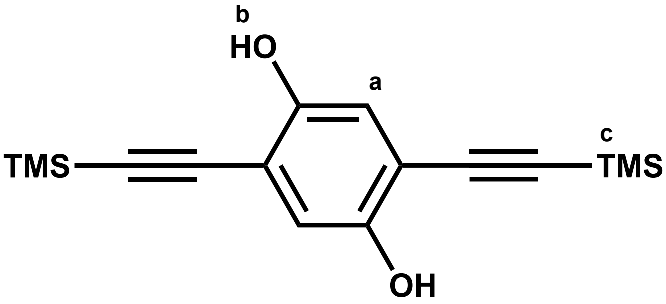

**S2** (1.00 g, 2.76 mmol, 1.00 eq.), CuI (0.053 g, 0.276 mmol, 0.10 eq.), and [PdCl$_2$(PPh$_3$)$_2$] (0.058 g, 0.083 mmol, 0.03 eq.) were combined under an argon atmosphere. Ethynyltrimethylsilane (0.97 mL, 6.91 mmol, 2.50 eq.), dry triethylamine (2.3 mL, 16.58 mmol, 6.00 eq.) and dry THF (25 mL) were added and the solution refluxed for 24 hours. $CH_2Cl_2$ (50 mL) and $NH_4OH$/EDTA (100 mL) were added, and the aqueous layer extracted with $CH_2Cl_2$ (2 x 50 mL). The organic phase was washed with water (100 mL) and saturated aqueous NaCl (100 mL), dried over $Na_2SO_4$, and the solvent removed *in vacuo*. Column chromatography (silica gel, gradient 100% petrol, then 100% $CH_2Cl_2$) was used to obtain the product as an off-white solid. Yield: 0.591 g, 71%. Mp 158 ˚C; $^1H$ NMR (400 MHz, $CDCl_3$) δ 6.90 (s, 2H, $H_a$), 5.44 (s, 2H, $H_b$), 0.27 (s, 18H, $H_c$); $^{13}C$ NMR (125 MHz, $CDCl_3$) δ 150.5, 116.7, 111.7, 104.2, 98.6, 0.0; IR (ATR): ν ($cm^{-1}$) 3453, 2958, 2900, 2146, 1418, 1247, 1191, 832, 756, 627; HRESI-MS ($CH_3OH$) *m/z* = 303.1204 [**S3**+H]$^+$ (calc. for $C_{16}H_{23}O_2Si_2$ 303.1231); Anal. Calc. for $C_{16}H_{23}O_2Si_2$•$0.1H_2O$: C, 63.15; H, 7.35; N, 0.00%. Found: C, 62.93; H, 7.43; N, 0.00%.

### 1.4 1,4-Diethynyl-2,5-bis(hexyloxy)benzene (S4)

The synthesis of this compound has previously been achieved by a number of groups through alkylation of a 1,4-benzenediol, followed by iodination or bromination, Sonogashira coupling of the ethynyltrimethylsilane, and eventual deprotection, to give the target compound in 13-38% overall yield.[5-7]

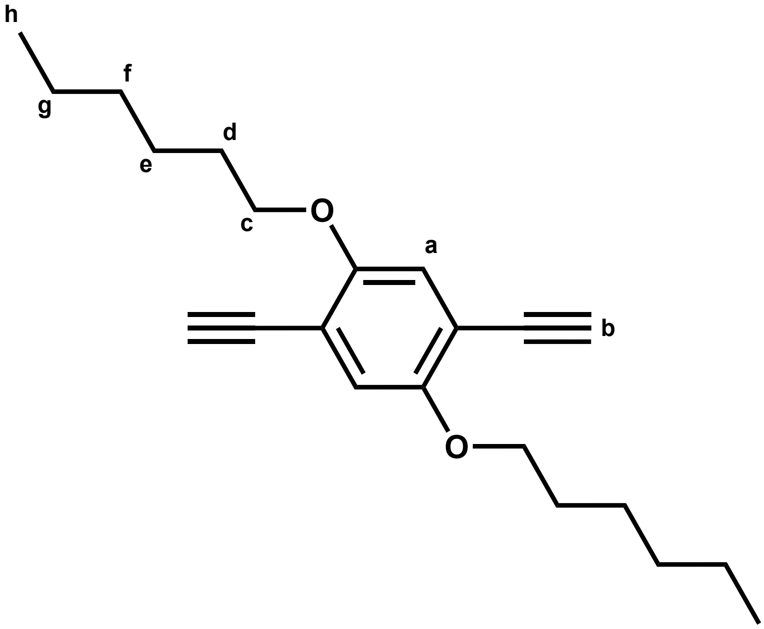

**S3** (0.25 g, 0.826 mmol, 1.00 eq.), 1-bromohexane (0.26 mL, 1.818 mmol, 2.20 eq.), and $K_2CO_3$ (0.343 g, 2.479 mmol, 3.00 eq.) were combined in DMF and stirred at 50 °C overnight (16 hours). The mixture was cooled to room temperature, poured into water (50 mL), and extracted with hexane (3 x 50 mL). The organic fraction was dried over $MgSO_4$ and the solvent removed *in vacuo* to give the pale yellow product. Column chromatography (silica gel, gradient 100% petrol, then 9:1 petrol/diethyl ether) was used to further purify the product. Yield: 0.136 g, 50%. Mp 68 ˚C; $^1H$ NMR (400 MHz, $CDCl_3$) δ 6.95 (s, 2H, $H_a$), 3.97 (t, *J* = 6.6 Hz, 4H, $H_c$), 3.32 (s, 2H, $H_b$), 1.80 (qt, *J* = 8.0 Hz, 4H, $H_d$), 1.47 (qt, *J* = 8.0 Hz, 4H, $H_e$), 1.37-1.31 (m, 8H, $H_{f/g}$), 0.90 (t, *J* = 7.0 Hz, 6H, $H_h$); $^{13}C$ NMR (125 MHz, $CDCl_3$) δ 154.1, 117.9, 113.4, 82.5, 79.9, 69.8, 31.7, 29.2, 25.7, 22.7, 14.2; IR (ATR): ν (cm$^{-1}$) 3279, 2938, 2853, 1744, 1497, 1467, 1383, 1272, 1216, 1027, 861, 645; HRESI-MS ($CH_3OH$) *m/z* = 349.2047 [**S4**+Na]$^+$ (calc. for $C_{22}H_{30}O_2Na$ 349.2138); Anal. Calc. for $C_{22}H_{30}O_2$: C, 80.94; H, 9.26; N, 0.00%. Found: C, 80.94; H, 9.34; N, 0.00%.

### 1.5 1,4-Di-(1-ethynyl-1′-(5-yl-ethynyl-2,2′-bipyridine)ferrocene)-2,5-bis(hexyloxy)benzene (difcbipy)

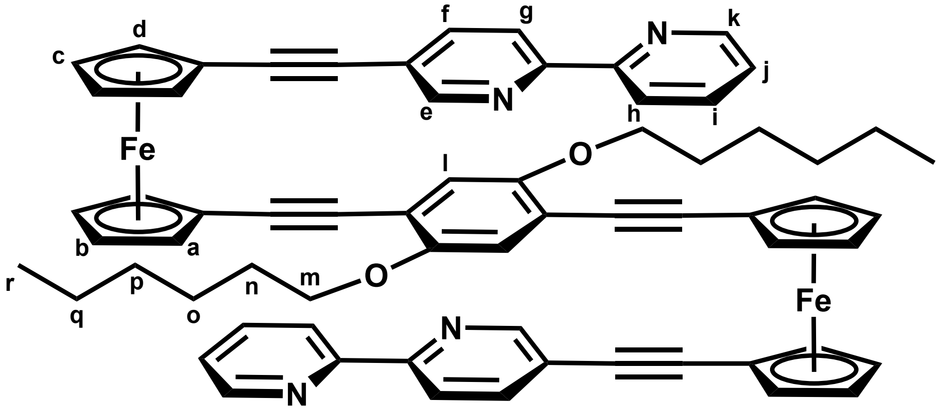

**S4** (0.050 g, 0.153 mmol, 1.00 eq.) and 1-(5-yl-ethynyl-2,2′-bipyridine)-1′-iodo-ferrocene[1] (0.225 g, 0.459 mmol, 3.00 eq.) were combined in diisopropylamine (10 mL), and degassed with argon. CuI (0.006 g, 0.031 mmol, 0.20 eq.), $[Pd(CH_3CN)_2Cl_2]$ (0.002 g, 0.009 mmol, 0.06 eq.), and $[PH(^tBu)_3]BF_4$ (0.005 g, 0.018 mmol, 0.12 eq.) were subsequently added under an argon atmosphere. The resulting mixture was irradiated in a microwave reactor for four hours at 100 °C (300 W). $CH_2Cl_2$ (50 mL) and $NH_4OH$/EDTA (50 mL) were added, and the aqueous layer extracted with $CH_2Cl_2$ (3 x 50 mL). The organic phase was washed with saturated aqueous NaCl (200 mL), dried over $Na_2SO_4$, and the solvent removed *in vacuo*. Column chromatography (silica gel, gradient 100% $CH_2Cl_2$, then 95:5 $CH_2Cl_2$/acetone, then 9:1 $CH_2Cl_2$/acetone) was used to obtain the desired product as an orange solid. Yield: 0.019 g, 12%. Mp 154 ˚C; $^1H$ NMR (400 MHz, $CDCl_3$) δ 8.68-8.65 (m, 4H, $H_{e/k}$), 8.40 (d, *J* = 8 Hz, 2H, $H_h$), 8.31 (d, *J* = 8 Hz, 2H, $H_g$), 7.81-7.76 (m, 4H, $H_{i/f}$), 7.28 (ddd, *J* = 8, 5, 1 Hz, 2H, $H_j$), 6.82 (s, 2H, $H_l$), 4.59 (t, *J* = 2 Hz, 4H, $H_a$ or $H_d$), 4.55 (t, *J* = 2 Hz, 4H, $H_a$ or $H_d$), 4.37 (t, *J* = 2 Hz, 4H, $H_b$ or $H_c$), 4.36 (t, *J* = 2 Hz, 4H, $H_b$ or $H_c$), 3.90 (t, *J* = 7 Hz, 4H, $H_m$), 1.79 (qt, *J* = 7 Hz, 4H, $H_n$), 1.51 (qt, *J* = 7 Hz, 4H, $H_o$), 1.39-1.31 (m, 8H, $H_{p/q}$), 0.90 (t, *J* = 7 Hz, 6H, $H_r$); $^{13}C$ NMR (125 MHz, $CDCl_3$) δ 155.8, 154.3, 153.6, 151.5, 149.4, 139.1, 137.0, 123.9, 121.5, 121.0, 120.3, 116.8, 114.0, 92.3, 92.1, 83.9, 83.6, 73.2, 73.1, 71.7, 71.3, 69.6, 67.7, 66.3, 31.8, 29.5, 25.9, 22.8, 14.3; IR (ATR): ν (cm$^{-1}$) 2921, 2856, 2211, 1587, 1508, 1435, 1216, 855, 819, 798, 492; HRESI-MS ($CH_3OH$) *m/z* = 1073.3117 [**difcbipy**+Na]$^+$ (calc. for $C_{66}H_{58}Fe_2N_4O_2Na$ 1073.3154); UV-Vis (acetone) $\lambda_{max}$ (ε/ L mol$^{-1}$ cm$^{-1}$): 368 (17900), 430 (4400); Anal. Calc. for $C_{66}H_{58}Fe_2N_4O_2 \bullet H_2O$: C, 74.16; H, 5.66; N, 5.24%. Found: C, 74.35; H, 5.72; N, 5.13%.

### 1.6 [Cu$_2$(difcbipy)(dimesbipy)$_2$](PF$_6$)$_2$

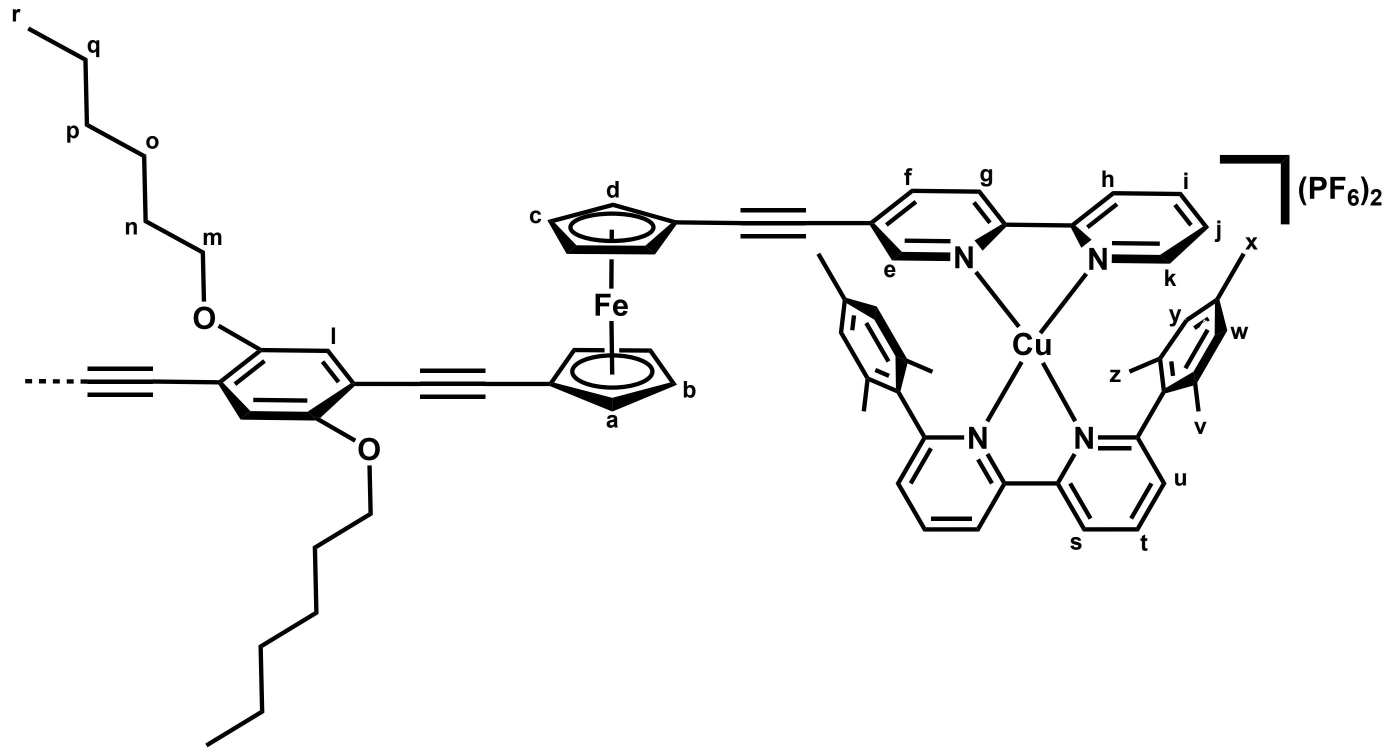

[Cu(CH$_3$CN)$_4$]PF$_6$ (57 mg, 0.152 mmol, 2.00 eq.) was dissolved in acetone (3 mL) and 6,6′-dimesityl-2,2′-bipyridine (60 mg, 0.152 mmol, 2.00 eq.), also dissolved in acetone (3 mL), was added. The mixture was stirred for 15 minutes to give a yellow solution. **Difcbipy** (80 mg, 0.076 mmol, 1.00 eq.) was dissolved in acetone (3 mL) and added to this solution. The mixture was stirred for 15 minutes, then filtered through a cotton wool plug and the solvent removed *in vacuo* to give the red product. Yield: 164 mg, 95%. Mp 134 ˚C; $^1$H NMR (400 MHz, CDCl$_3$) δ 8.48 (d, *J* = 8 Hz, 4H, H$_s$), 8.23 (t, *J* = 8 Hz, 4H, H$_t$), 8.10-8.07 (m, 4H, H$_e$ and H$_k$), 7.95-7.82 (m, 8H, H$_{f/g/h/i}$), 7.49 (d, *J* = 8 Hz, 4H, H$_u$), 7.36 (t, *J* = 6 Hz, 2H, H$_j$), 6.88 (s, 2H, H$_l$), 6.18 (s, 4H, H$_w$ or H$_y$), 6.10 (s, 4H, H$_w$ or H$_y$), 4.60 (s br., 4H, H$_a$ or H$_d$), 4.57 (s br., 4H, H$_a$ or H$_d$), 4.43 (s br., 4H, H$_b$ or H$_c$), 4.37 (s br., 4H, H$_b$ or H$_c$), 3.92 (t, *J* = 6 Hz, 4H, H$_m$), 1.86 (s, 12H, H$_x$), 1.84-1.79 (m, 4H, H$_n$), 1.75 (s, 12H, H$_v$ or H$_z$), 1.73 (s, 12H, H$_v$ or H$_z$), 1.50 (qt, *J* = 8 Hz, 4H, H$_o$), 1.36-1.28 (m, 8H, H$_{p/q}$), 0.86 (t, *J* = 7 Hz, 6H, H$_r$); $^{13}$C NMR (100 MHz, CDCl$_3$) δ 158.5, 153.6, 152.1, 150.5, 149.6, 148.8, 147.9, 138.9, 138.6, 138.0, 137.3, 137.2, 134.7, 134.6, 127.5, 127.4, 127.0, 125.3, 122.8, 121.0, 120.4, 120.4, 117.0, 114.0, 95.3, 92.7, 83.1, 82.0, 73.6, 73.2, 72.3, 71.7, 69.6, 68.0, 67.1, 64.8, 31.6, 29.4, 25.8, 25.7, 22.7, 20.7, 20.2, 20.2, 14.2; IR (ATR): ν (cm$^{-1}$) 2918, 2856, 1509, 833, 556; HRESI-MS (CH$_3$OH/CHCl$_3$): *m/z* = 981.3261 [Cu$_2$(**difcbipy**)(**dimesbipy**)$_2$]$^{2+}$ (calc. for C$_{122}$H$_{114}$Cu$_2$Fe$_2$N$_8$O$_2$ 981.3187), *m/z* = 2107.6128 [Cu$_2$(**difcbipy**)(**dimesbipy**)$_2$]PF$_6^+$ (calc. for C$_{122}$H$_{114}$Cu$_2$Fe$_2$N$_8$O$_2$PF$_6$ 2107.6021); UV-Vis (acetone) λ$_{max}$ (ε/ L mol$^{-1}$ cm$^{-1}$): 367 (68200), 460 (22100); Anal. Calc. for C$_{122}$H$_{114}$Cu$_2$Fe$_2$N$_8$P$_2$F$_{12}$•0.5H$_2$O: C, 64.78; H, 5.12; N, 4.95%. Found: C, 64.47; H, 5.45; N, 4.83%.

## 2 NMR spectra

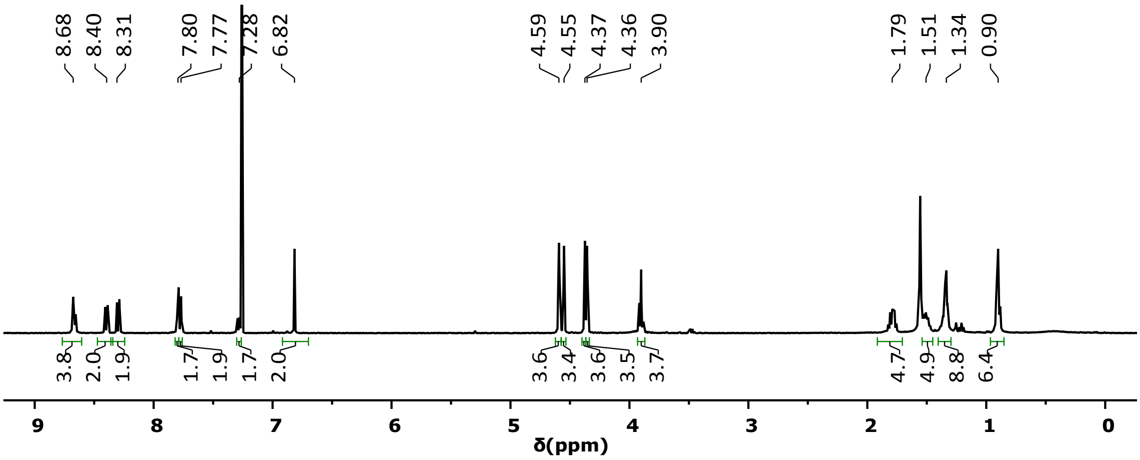

**Figure S1** $^1$H NMR spectrum (CDCl$_3$, 298 K, 400 MHz) of **difcbipy**.

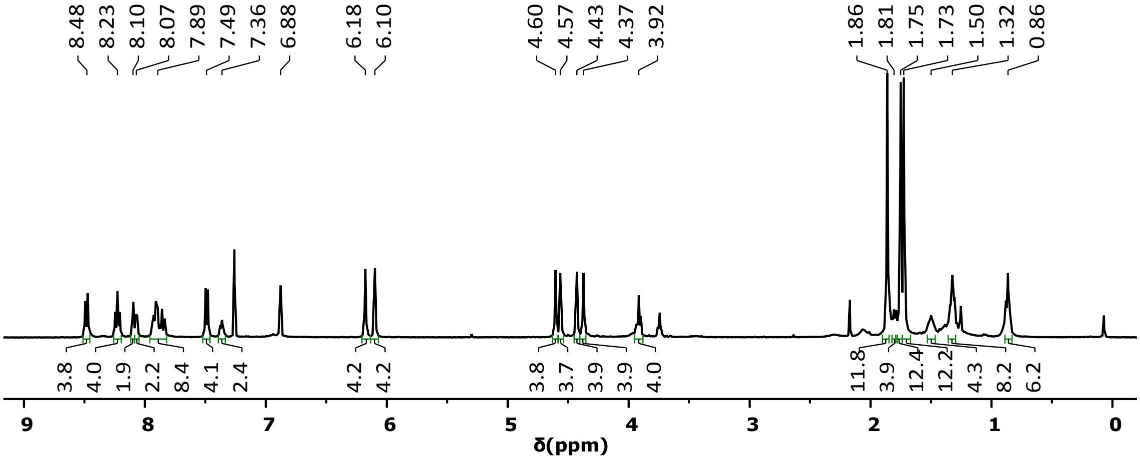

**Figure S2** $^1$H NMR spectrum (CDCl$_3$, 298 K, 400 MHz) of **[Cu$_2$(difcbipy)(dimesbipy)$_2$](PF$_6$)$_2$**.

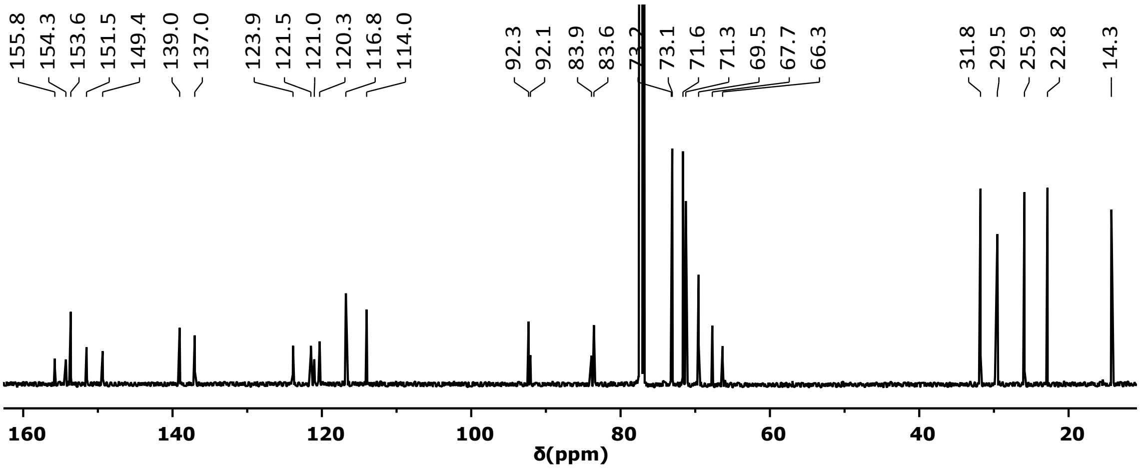

**Figure S3** $^{13}$C NMR spectrum (CDCl$_3$, 298 K, 125 MHz) of **difcbipy**.

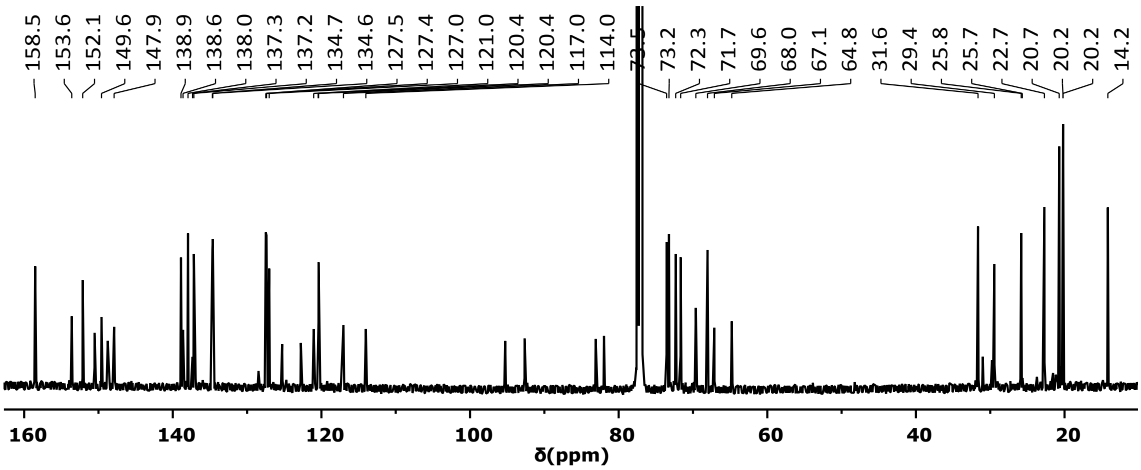

**Figure S4** $^{13}$C NMR spectrum ($CDCl_3$, 298 K, 100 MHz) of **[Cu$_2$(difcbipy)(dimesbipy)$_2$](PF$_6$)$_2$**.

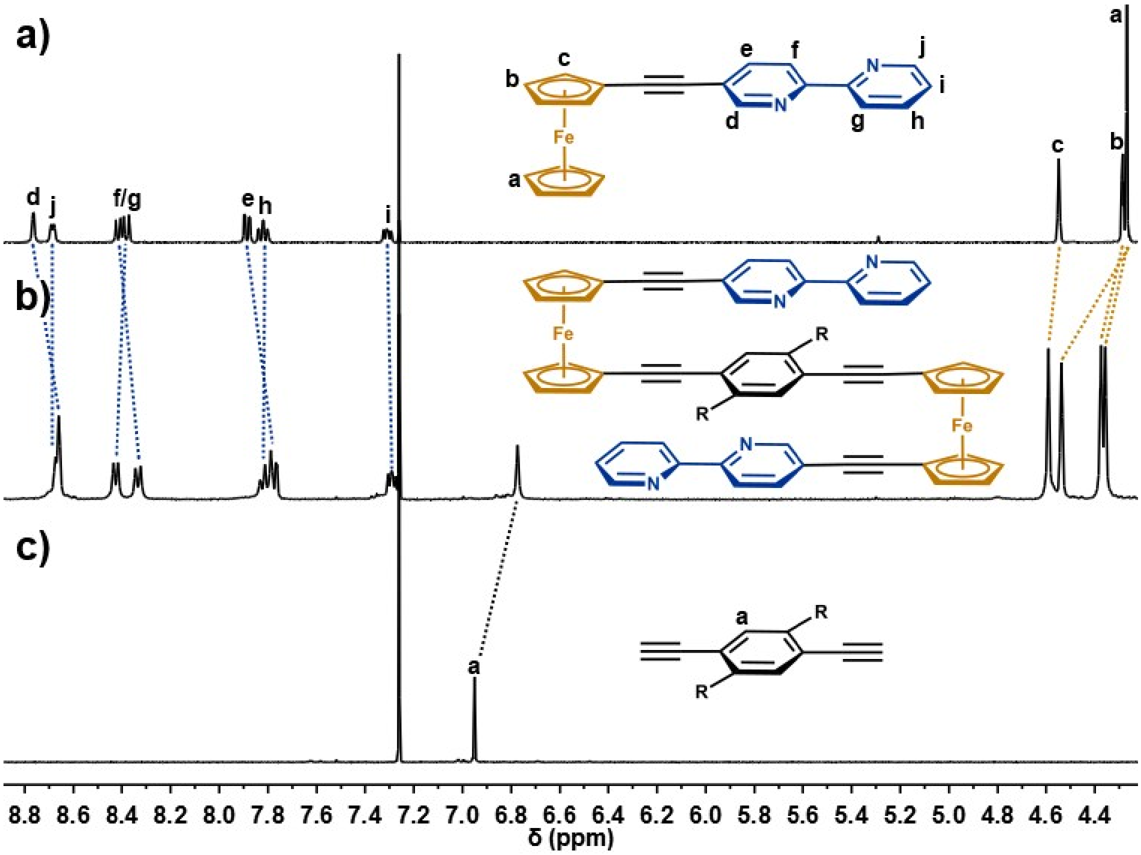

**Figure S5** $^1$H NMR spectra ($CDCl_3$, 298 K, 400 MHz) of a) the mono-substituted model compound 1-(5-yl-ethynyl-2,2'-bipyridine)ferrocene, b) the triple tiered actuator **difcbipy**, and c) the intermediate middle tier **S4**. **R** in all cases is the hexyloxy solubilising chain.

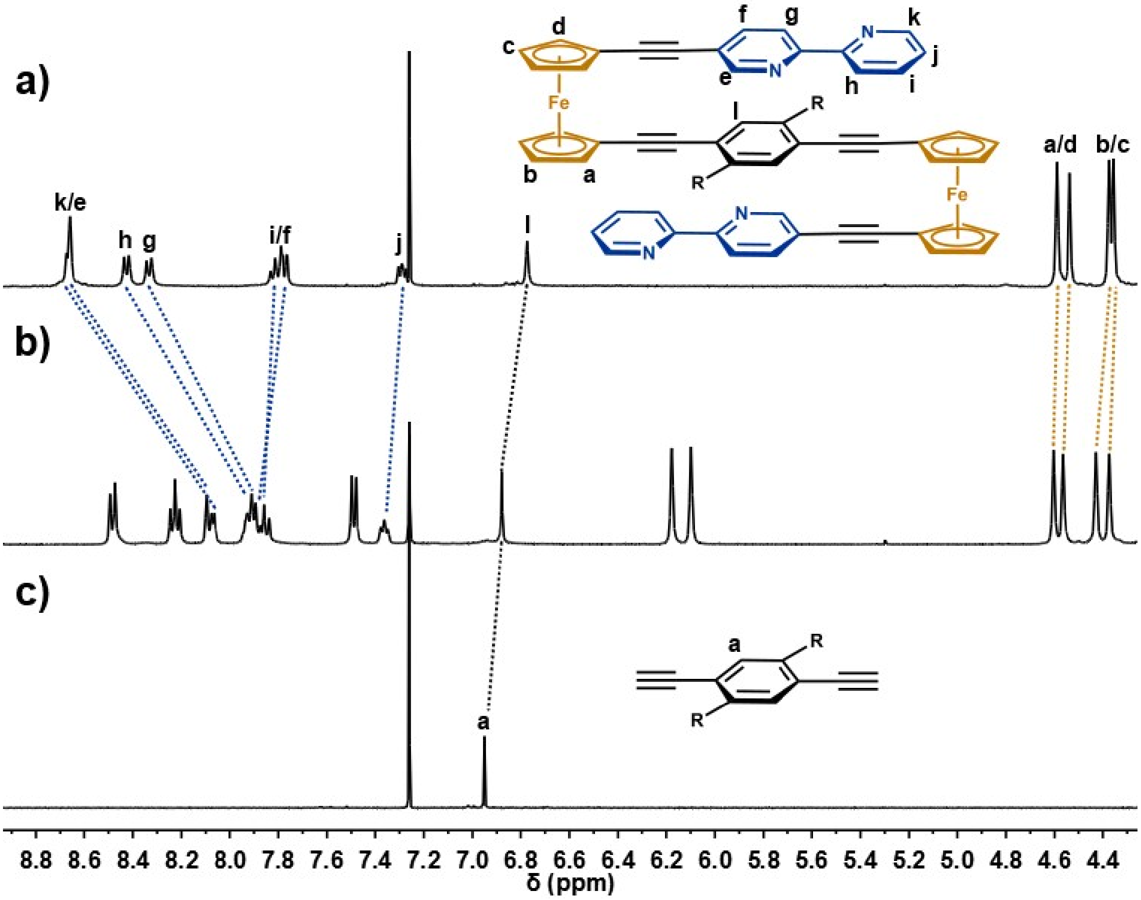

**Figure S6** $^1$H NMR spectra ($CDCl_3$, 298 K, 400 MHz) of a) the contracted triple-tiered actuator **difcbipy**, b) the extended Cu(I) complexed actuator [$Cu_2$(**difcbipy**)(**dimesbipy**)$_2$]($PF_6$)$_2$, and c) the intermediate middle tier **S4**. **R** in all cases is the hexyloxy solubilising chain.

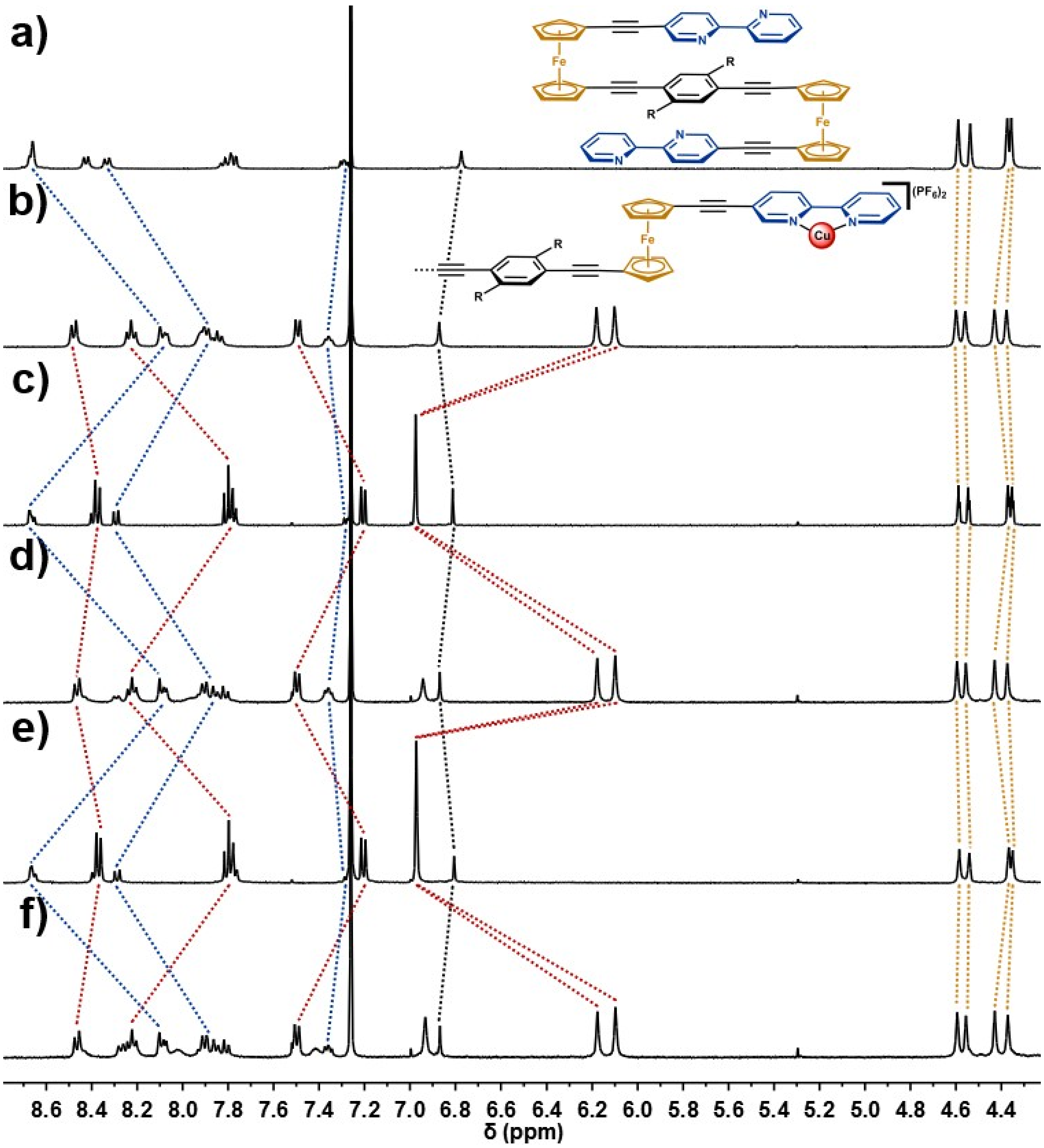

**Figure S7** Stacked $^1$H NMR spectra (CDCl$_3$, 298 K, 400 MHz) of a) the contracted triple-tiered actuator **difcbipy**, b) the extended Cu(I) complex [Cu$_2$(**difcbipy**)(**dimesbipy**)$_2$](PF$_6$)$_2$, c) [Cu$_2$(**difcbipy**)(**dimesbipy**)$_2$](PF$_6$)$_2$ after the addition of 2 eq. of cyclam, d) after the subsequent addition of 2 eq. of Cu(I), e) after the addition of a further 2 eq. of cyclam, and f) after the addition of a further 2 eq. Cu(I). Only select bipyridyl proton signal shifts are traced in order to aid clarity.

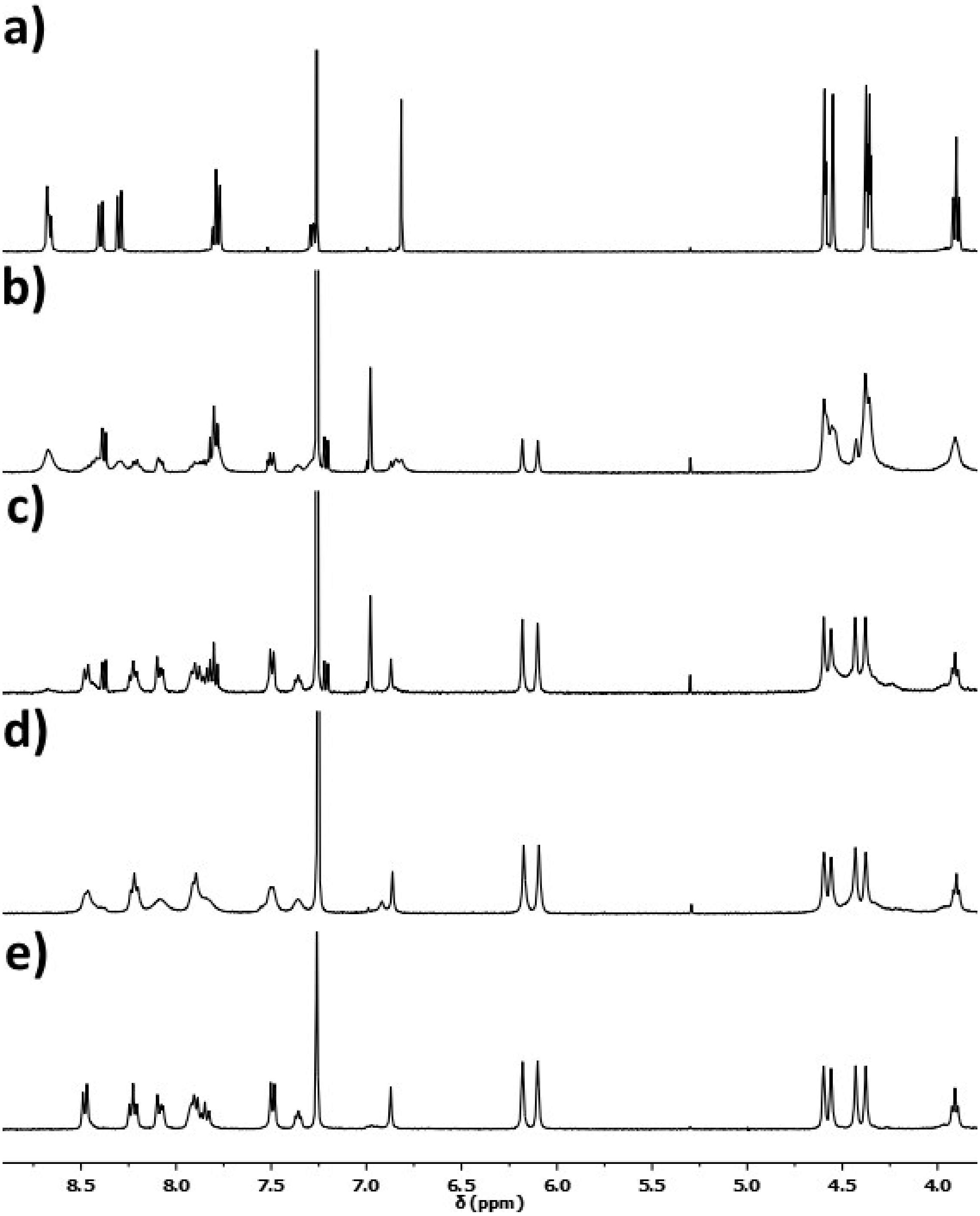

**Figure S8** Stacked $^{1}$H NMR spectra ($CDCl_3$, 298 K, 400 MHz) of a) the contracted triple-tiered actuator **difcbipy**, b) **difcbipy** with 0.5 eq. of [Cu(**dimesbipy**)($CH_3CN$)$_2$]$PF_6$ added, c) **difcbipy** with 1.0 eq. of [Cu(**dimesbipy**)($CH_3CN$)$_2$]$PF_6$ added, d) **difcbipy** with 1.5 eq. of [Cu(**dimesbipy**)($CH_3CN$)$_2$]$PF_6$ added, and e) **difcbipy** with 2.0 eq. of [Cu(**dimesbipy**)($CH_3CN$)$_2$]$PF_6$ added.

## 3 Mass spectrum of [$Cu_2$(difcbipy)(dimesbipy)$_2$]($PF_6$)$_2$

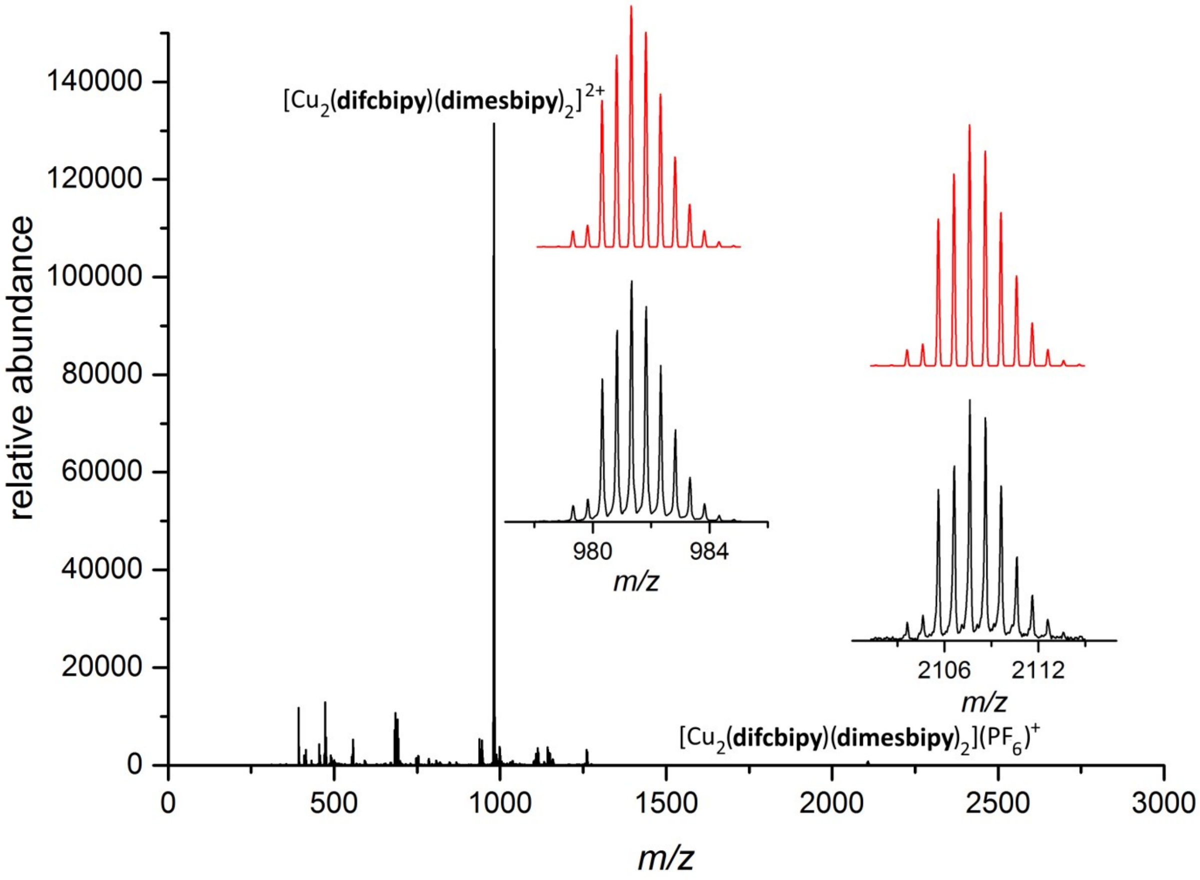

**Figure S9** Full mass spectrum ($CH_3OH/CHCl_3$) of complex [$Cu_2$(**difcbipy**)(**dimesbipy**)$_2$]($PF_6$)$_2$ with relevant peaks annotated. The calculated (red trace) and experimental (black trace) isotope patterns of each peak is inset.

# 4 UV-Vis spectra

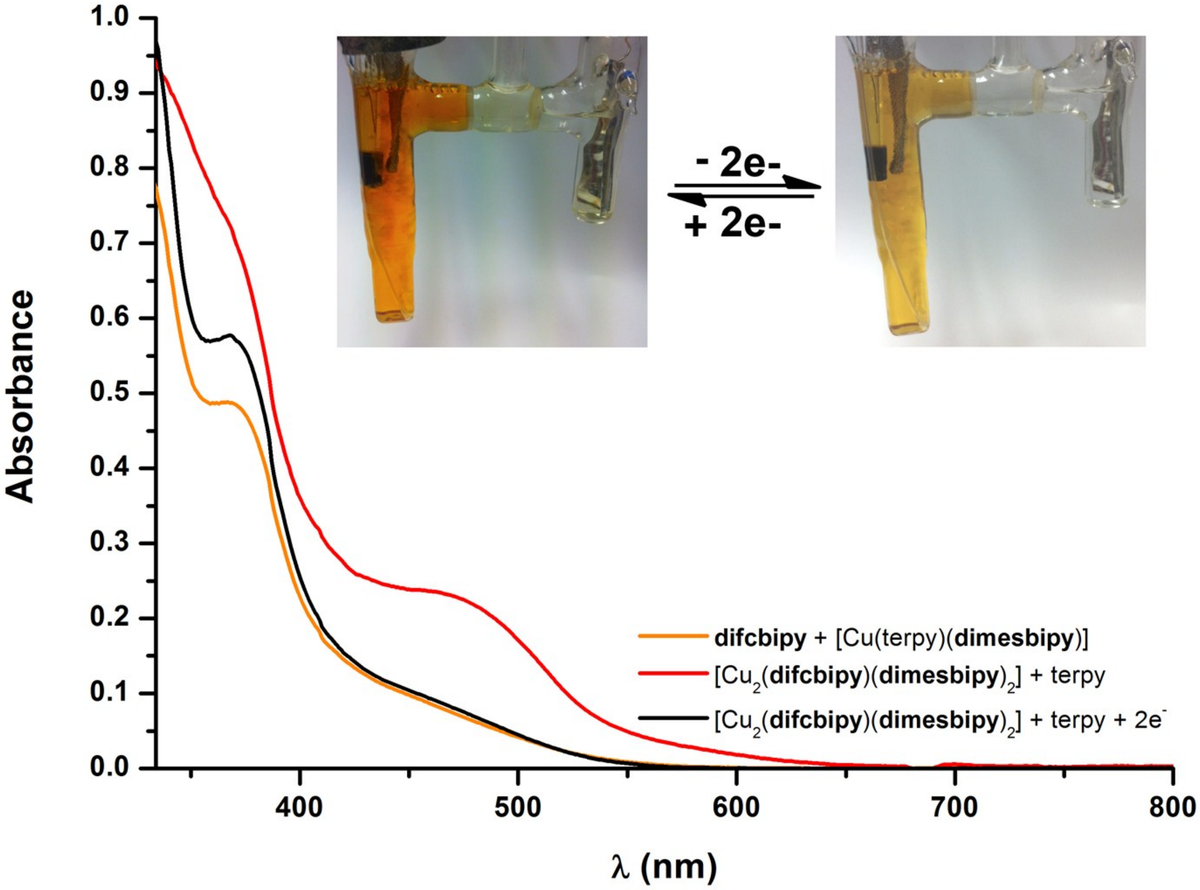

**Figure S10** UV-Vis spectra of the contracted actuator **difcbipy** in the presence of [Cu(**terpy**)(**dimesbipy**)]$PF_6$, the extended actuator [$Cu_2$(**difcbipy**)(**dimesbipy**)$_2$]$(PF_6)_2$ in the presence of terpyridine, and the complex [$Cu_2$(**difcbipy**)(**dimesbipy**)$_2$]$(PF_6)_2$ in the presence of terpyridine after the oxidation of the Cu(I) to Cu(II). Inset is the colour change seen during bulk electrolysis of a 1 mM solution.

## 5 Electrochemistry

Cyclic voltammetric (CV) experiments in acetone were performed at 20 ˚C on solutions degassed with argon. A three-electrode cell was used with Cypress Systems 1.4 mm diameter glassy carbon working, Ag/AgCl reference and platinum wire auxiliary electrodes. The solution was ~$10^{-3}$ M in electroactive material and contained 0.1 M $Bu_4NPF_6$ as the supporting electrolyte. Voltammograms were recorded with the aid of a Powerlab/4sp computer-controlled potentiostat. Potentials are referenced to the reversible formal potential (taken as $E^\circ$ = 0.00 V) for the decamethylferrocene $[Fc^*]^{+/0}$ process.[8] Under the same conditions, $E^\circ$ calculated for $[FcH]^{+/0}$ was 0.49 V (acetone).[9] Bulk electrolysis experiments were undertaken in a three-compartment cell in which the working and auxiliary compartments were separated by two fine frits to minimize mixing of the solutions. The experimental reference electrode was a AgCl-coated Ag wire prepared by anodic electrolysis of the wire in 1 M HCl. Spectroelectrochemical experiments were performed in acetone/0.1 M $Bu_4NPF_6$ solution in an OTTLE cell (pathlength 0.5 mm) with Pt working and auxiliary, and Ag reference electrodes.

**Table S1** Electrochemical data for the triple-tiered ferrocene system (**difcbipy**), its Cu(I) complex ([$Cu_2$(**difcbipy**)(**dimesbipy**)$_2$]$(PF_6)_2$), and the Cu(II) complex [Cu(**dimesbipy**)(**terpy**)]$(PF_6)_2$.

| Compound | $E^\circ$ (V) (acetone)[a] | |
|---|---|---|
| | $Cu^{II/I}$ | $Fc^{+/0}$ |
| **difcbipy** | - | 0.73 |
| [$Cu_2$(**difcbipy**)(**dimesbipy**)$_2$]$(PF_6)_2$ | 0.66 | 0.80 |
| [Cu(**dimesbipy**)(**terpy**)]$(PF_6)_2$ | -0.15 | - |

[a] $1\times10^{-3}$ M in analyte, 0.1 M $Bu_4NPF_6$, referenced to $[Fc^*]^{+/0}$ = 0.00 V.

# 6 Computational Details

Computational modelling was performed with the Gaussian 09 software package[10] using the CAM-B3LYP[11] functional and 6-31G(d) basis set. A DMF solvent field was implemented using an integral equation formalism polarisable continuum model (IEF-PCM) self-consistent reaction field (SCRF)[12] with the default solvent parameters provided by Gaussian. This methodology has been noted to give effective predictive ability in prior studies.[1,13] The ligand **difcbipy** was modelled in both the open and closed forms while the Cu complex $[Cu_2($**difcbipy**$)($**dimesbipy**$)_2]^{2+}$ was modelled only in the open form. Simulated Raman spectra were generated utilising GaussSum v2.2 software,[14] with a scaling factor of 0.95. The mean absolute deviations (MAD), generated using well established methods,[15] between experimental and simulated Raman bands in the alkyne systems were reasonable at between 7 and 10 cm$^{-1}$ (**Figure S11** and **Table S2**). The potential energy surface scan of the ferrocene dihedral angle (α) was accomplished by freezing the dihedral angle at various values and allowing the rest of the molecule to relax to its lowest energy configuration. The structure at which $\alpha = 180°$ was taken to be the zero energy point (as this could be calculated for all systems) and the energy of the other dihedrals was calculated relative to this to allow Figure S13 and Figure S15 to be produced.

## 6.1 Raman Details

FT-Raman spectra were collected on powder samples using a Bruker MultiRam spectrometer. The excitation source was a Nd:YAG laser with an excitation wavelength of 1064 nm. Raman photons were measured with a liquid nitrogen-cooled D418T germanium detector. Spectra were collected with 128 scans, with laser power of 50 mW and spectral resolution of 1 cm$^{-1}$.

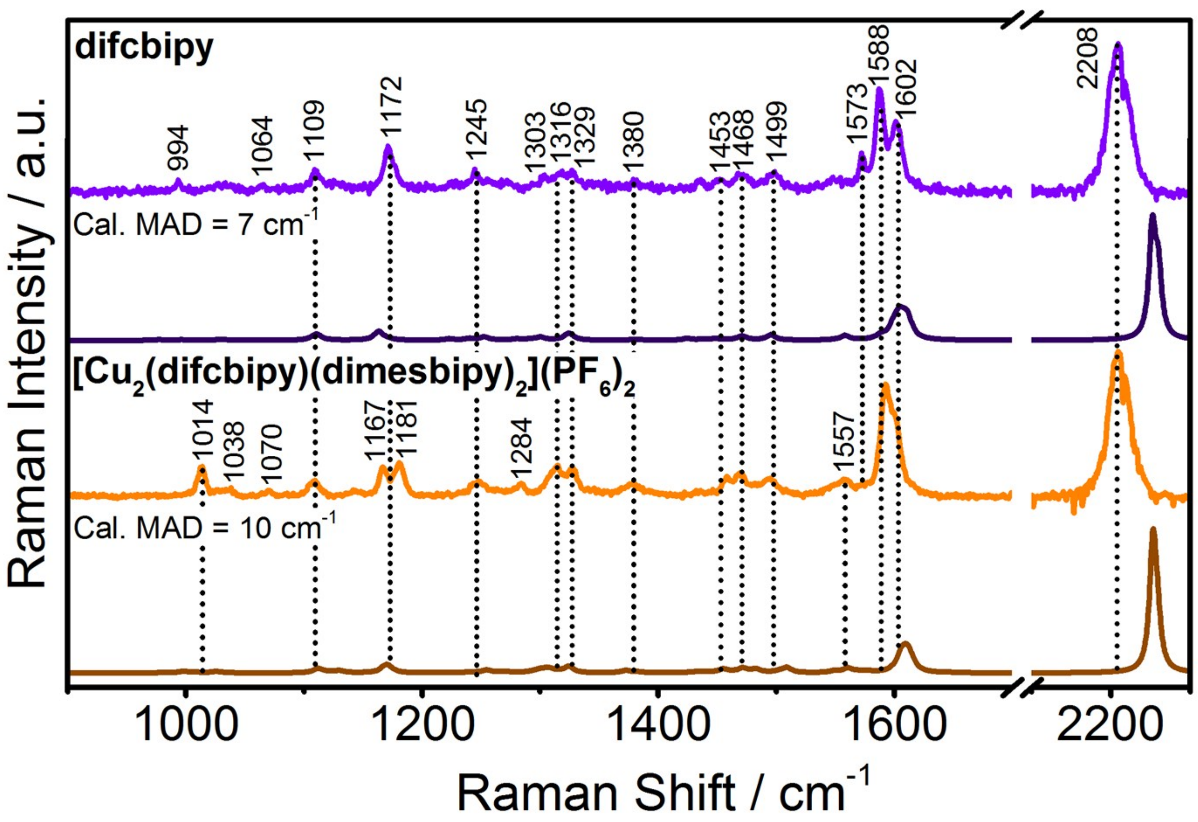

**Figure S11** Experimental and calculated Raman spectra. FT-Raman was collected at an excitation of 1064 nm. Calculated data is scaled by 0.95 to account for anharmonicity.

**Table S2** FT-Raman data and band assignments. Data was collected at an excitation of 1064 nm.

| Raman Shift / cm$^{-1}$ | | Assignment |
|---|---|---|
| **difcbipy** | **[Cu$_2$(difcbipy)(diMesbipy)$_2$](PF$_6$)$_2$** | |
| 2208 | 2210 | C≡C |
| 1602 | 1602 | linker |
| 1588 | 1593 | bipy |
| 1573 | | bipy |
| 1549 | 1557 | linker |
| 1499 | 1495 | Cp/bipy |
| 1468 | 1470 | Cp-linker-Cp |
| 1453 | 1458 | Cp/bipy |
| 1436 | | bipy |
| 1380 | 1379 | (Cp/bipy)$_2$ |
| 1329 | 1329 | Cp-linker-Cp |
| 1316 | 1315 | Cp/bipy |
| 1303 | | Cp/bipy |
| | 1284 | Ph H-wag |
| 1245 | | Cp-linker-Cp |
| | 1181 | Cp/bipy |
| 1172 | 1167 | Cp-linker-Cp |
| 1109 | 1109 | Cp H-wag |
| 1064 | 1070 | Cp-linker-Cp |
| | 1038 | Cp H-wag |
| 994 | 1014 | bipy breathing |

Ground state Raman spectra are dominated by bipy and C≡C based modes at ~1580 and 2210 cm$^{-1}$. A number of spectroscopic shifts are observed between **difcbipy** and the complexed [Cu$_2$(**difcbipy**)(**dimesbipy**)$_2$]$^{2+}$ species: on complexation the 994 cm$^{-1}$ bipy breathing mode shifts to 1014 cm$^{-1}$, the 1172 cm$^{-1}$ mode splits to 1167 and 1181 cm$^{-1}$, and the 1580 cm$^{-1}$ bipy mode region becomes dominated by the stronger 1593/1602 cm$^{-1}$ bands. These spectroscopic variations are consistent with analogous compounds in the literature, specifically the previously reported monoferrocene system.[13]

## 6.2 Ground State Geometry Scans

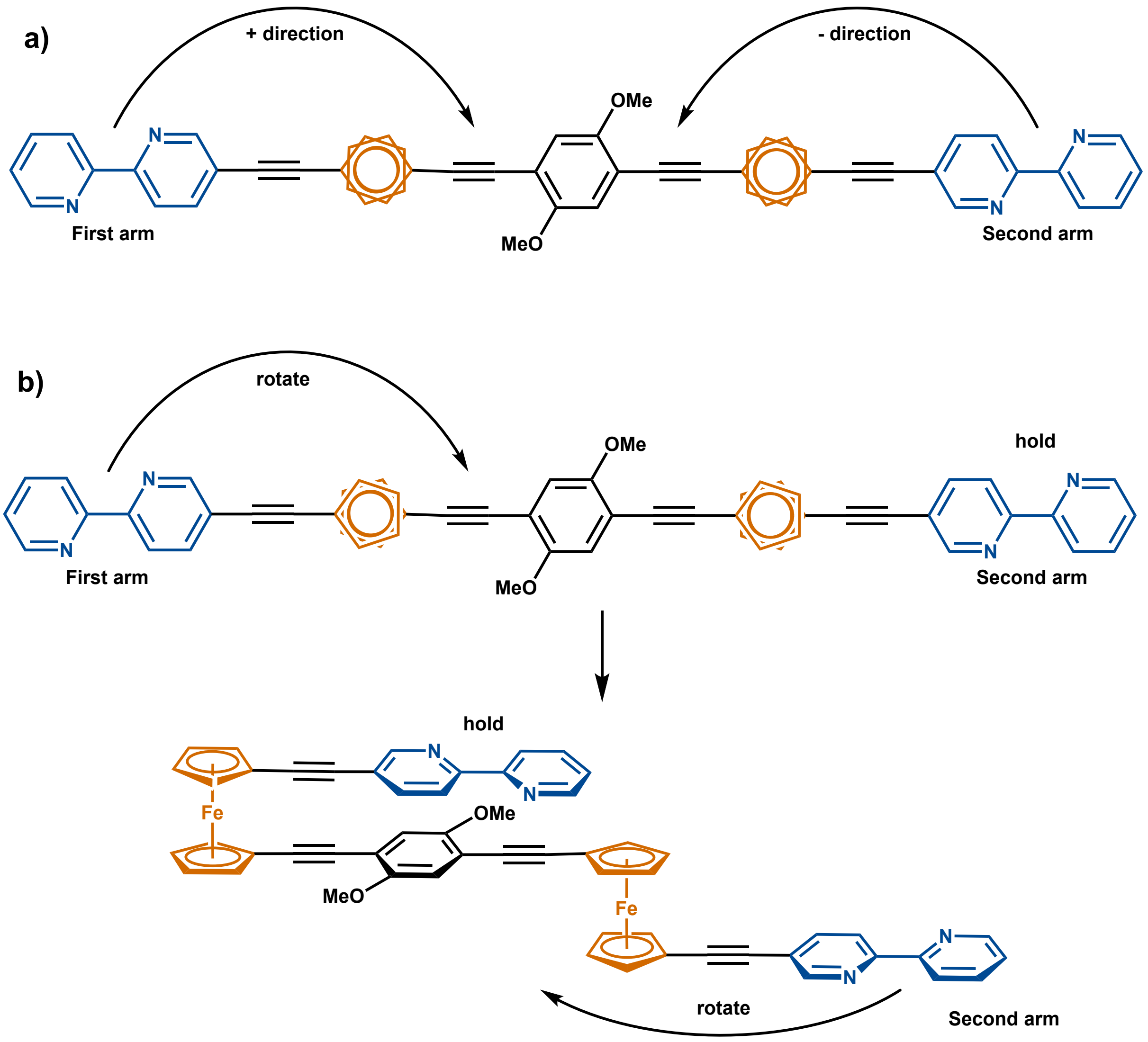

**Figure S12** Definitions implemented for geometry scans in this study. a) rotating both "arms" at the same time and b) rotating the first arm while holding the second arm fixed then fixing the first arm and roating the second arm.

To model the ground state potential energy surface, an optimised open structure was generated for both **difcbipy** and [Cu$_2$(**difcbipy**)(**dimesbipy**)$_2$]$^{2+}$ species. Previous studies have shown a CAM-B3LYP/6-31G(d) computational approach to give good approximations for such systems hence it was implemented here.[1,13] At specific intervals of rotation around the Fc unit, the energy profile of each species was interrogated. Geometry optimisations were attained for **difcbipy** due to logical identification of a local lowest energy state; while for [Cu$_2$(**difcbipy**)(**dimesbipy**)$_2$]$^{2+}$ inappropriate reorganisation of the metallic co-ordination sphere occurred such that single point energies at the various rotation intervals are used, as implemented previously.[1] To account for various degrees of freedom, ‘first’ and ‘second arms are defined. An energetic map is gathered where the ‘first’ and ‘second’ arms are moved in an identical direction towards the stacked α = 0° motif and is labelled below as ‘both arms’. Data was also gathered where the ‘first arm’ is moved towards α = 0° while the ‘second arm’ remains at α = 180° (defined ‘first arm’). In a continuous fashion the ‘second arm’ was then moved towards α = 0°, where the ‘first arm’ remained, to allow an energetic map of a stepwise stacking behaviour (defined as ‘second arm’).

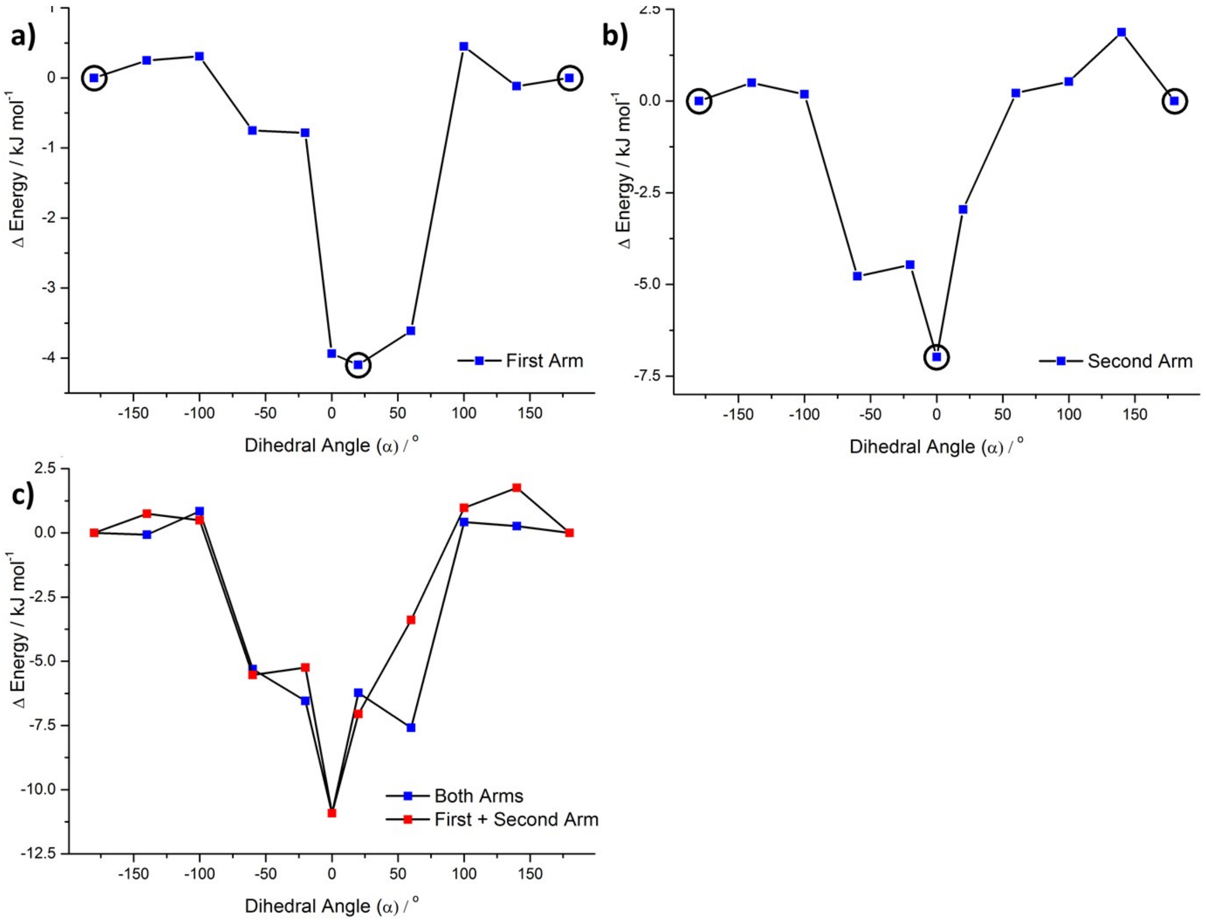

**Figure S13** DFT geometry scans of a) 'first' arm, b) 'second' arm and c) ‘both’ arms for **difcbipy**. Definitions are included in Figure S12. Non-equivalent circled structures are shown below in Figure S14.

Geometry scans for single and dual arm movements indicate a decrease in total energy for **difcbipy**, where a ‘global’ minimum is achieved at α = 0°, or the fully π-stacked arrangement. To validate, summation of ‘first’ and ‘second’ arm movements yields an energy profile consistent with that of the ‘both’ arms scan. A Boltzmann distribution of the ~10.5 kJ mol$^{-1}$ energy preference predicts greater than 98% of molecules will favour the stacked arrangement at room temperature.

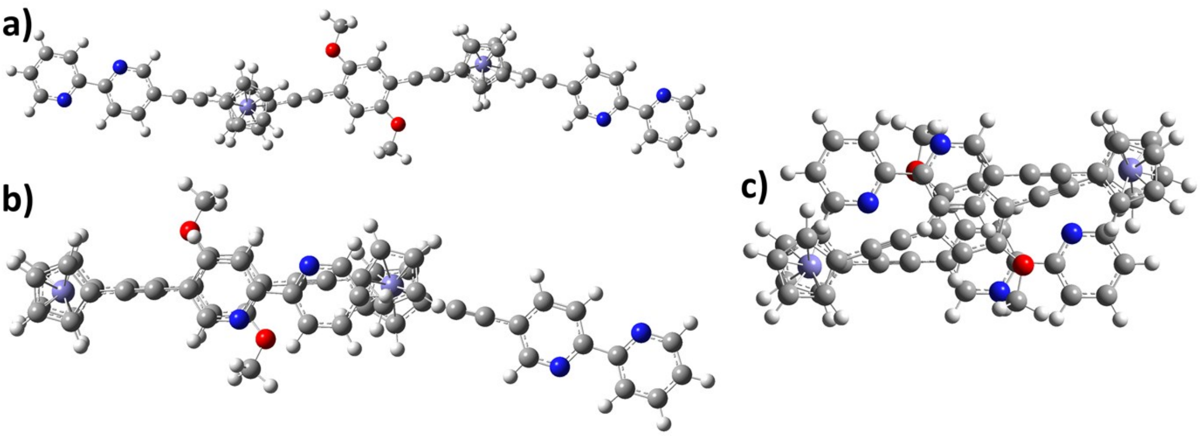

**Figure S14**. Structures for **difcbipy** at a) ±180°, b) 0° 'first' arm and c) 0° both arms. Angles denote starting angle, where optimisation procedure navigates to a lower energy state in 'slip-stacked' arrangements.

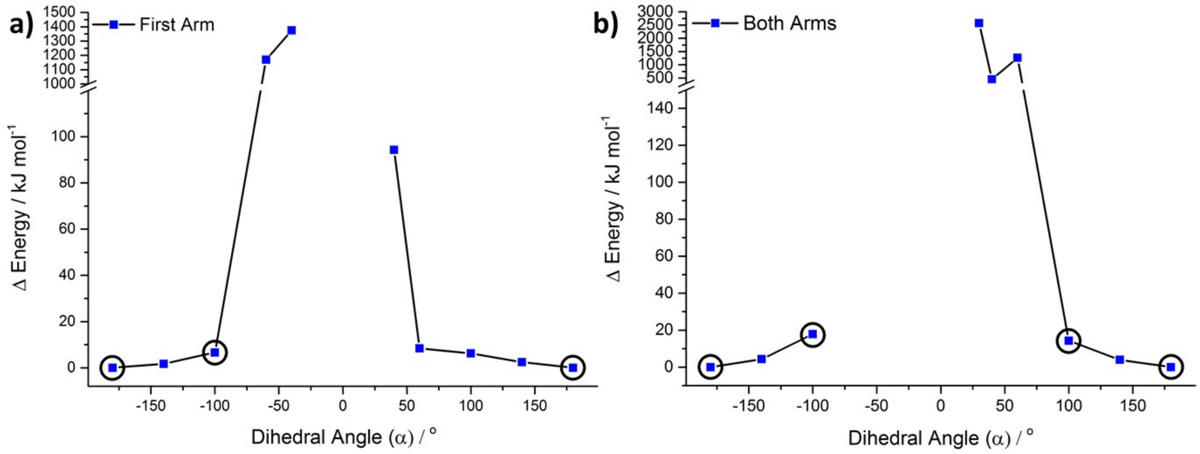

**Figure S15** DFT geometry scans of a) 'first' arm and b) 'second' arm for **[Cu$_2$(difcbipy)(diMesbipy)$_2$]$^{2+}$**. Definitions are included in Figure S12. Non-equvalent circled structures are shown below in Figure S16.

Complexation with [Cu(**dimesbipy**)]$^+$ shows vast increases of energies at values where α ≤ 100° while convergence issues become apparent at small α values approaching 0°. These results indicate the vast steric constraints of the metallated bipy arms. With rotation of both arms a more rapid increase of energy is observed compared to that of the 'first' arm, resulting in convergence issues at larger α.

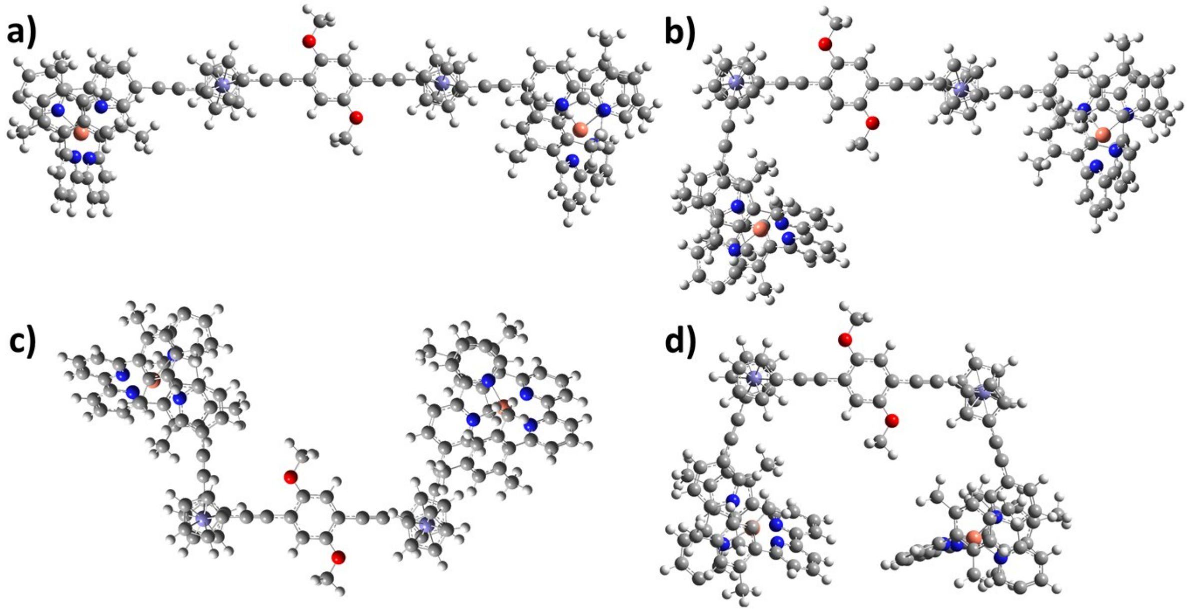

**Figure S16** Structures for [Cu$_2$(**difcbipy**)(**diMesbipy**)$_2$]$^{2+}$ at a) ±180$^o$, b) -100$^o$ 'first' arm, c) 100$^o$ 'both' arms and d) -100$^o$.

## 7 X-ray crystallography and data refinement details

The structure of **difcbipy** was collected on an Agilent Technologies SuperNova diffractometer with an Atlas detector using Cu Kα radiation (1.54184 Å) at low temperature (100 K). SADABS[16] was used for absorption correction. The structure was solved by direct methods using SHELXS within the X-Seed software package[17] and refined against F$^2$ using anisotropic thermal displacement parameters for all non-hydrogen atoms using SHELXL-97[18] software. Hydrogen atoms were placed in calculated positions and refined using a riding model. Additional information can be found in the crystallographic information file, CCDC number 1527569.

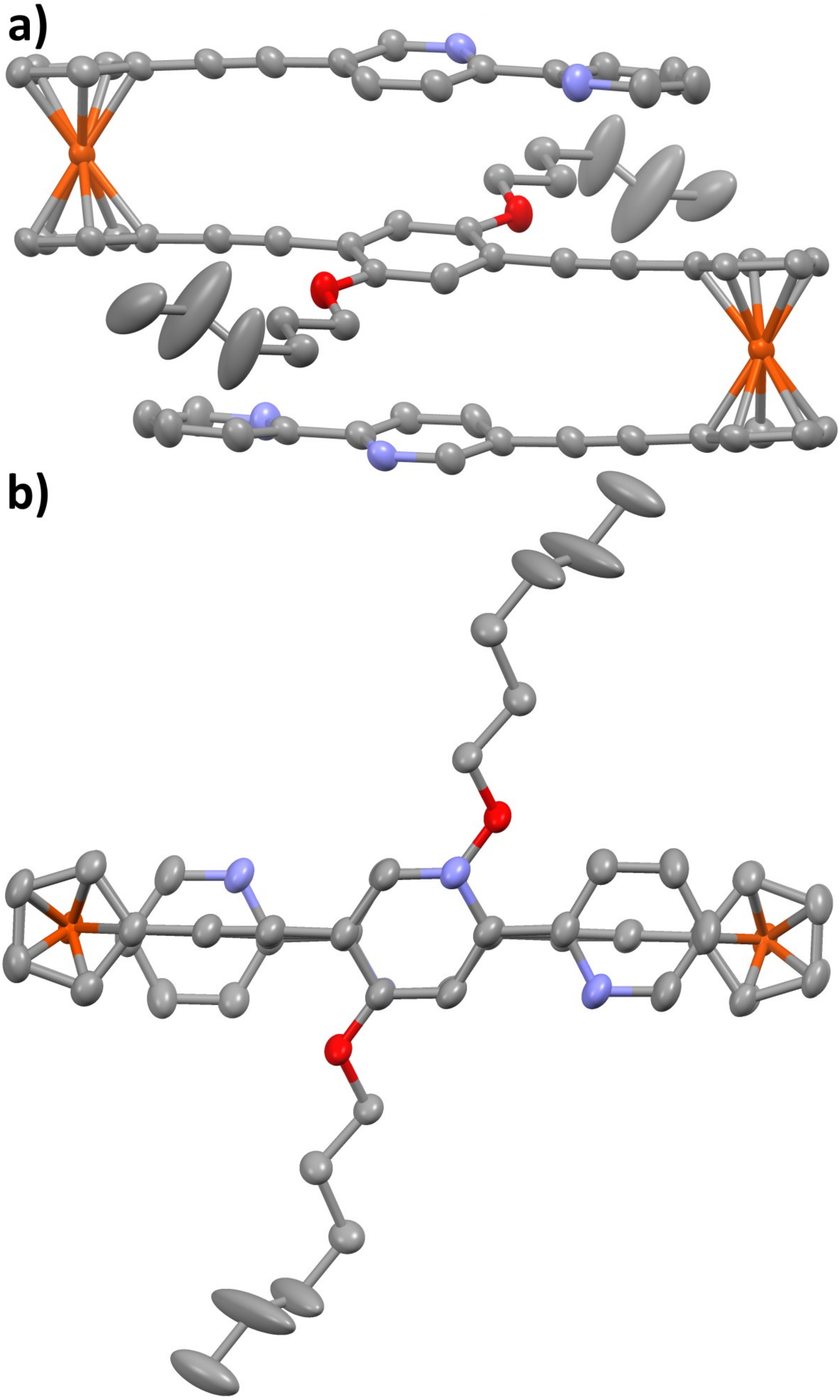

**Figure S17** One of the two molecules within the unit cell of **difcbipy** seen from a) the side and b) top down. Thermal ellipsoids are shown at the 50% probability level and protons are omitted for clarity.

## 7.1 Crystal Information Table

| Compound | **difcbipy** | |
|---|---|---|
| CCDC | 1527569 | |
| Empirical formula | $C_{66}H_{58}Fe_2N_4O_2$ | |
| Formula weight | 1050.86 | |
| Crystal system | Triclinic | |
| Space group | *P*-1 | |
| Unit cell dimensions | a = 9.9444(3) Å | α = 91.103(3)˚ |
| | b = 11.1804(3) Å | β = 90.102(3)˚ |
| | c = 23.4759(9) Å | γ = 93.933(3)˚ |
| Volume | 2603.46(15) Å$^3$ | |
| Z | 2 | |
| Density (calculated) | 1.341 Mg/m$^3$ | |
| Absorption coefficient | 4.861 mm$^{-1}$ | |
| F(000) | 1100 | |
| Crystal size | 0.2563 x 0.1763 x 0.1115 mm$^3$ | |
| Theta range for data collection | 3.752 to 73.366˚ | |
| Index ranges | -12<=h<=8, -13<=k<=13, -29<=l<=29 | |
| Reflections collected | 38202 | |
| Independent reflections | 10232 [R(int) = 0.0682] | |
| Completeness | 97.6% | |
| Data / restraints / parameters | 10232 / 0 / 669 | |
| Goodness-of-fit on F$^2$ | 1.047 | |
| Final R indices [I>2sigma(I)] | R1 = 0.0748, wR2 = 0.2001 | |
| R indices (all data) | R1 = 0.0944, wR2 = 0.2190 | |
| Largest diff. peak and hole | 1.51 and -0.72 e.Å$^{-3}$ | |

# 8 References

[1] S. Ø. Scottwell, A. B. S. Elliott, K. J. Shaffer, A. Nafady, C. J. McAdam, K. C. Gordon and J. D. Crowley, *Chem. Commun.*, **2015**, *51*, 8161-8164.

[2] T. Shiraki, S. Haraguchi, Y. Tsuchiya and S. Shinkai, *Chem. - Asian J.,* **2009**, *4*, 1434-1441.

[3] R. H. Pawle, A. Agarwal, S. Malveira, Z. C. Smith and S. W. Thomas, *Macromolecules,* **2014**, *47*, 2250-2256.

[4] R. Subramanian and F. Johnson, *J. Org. Chem.,* **1985**, *50*, 5430-5432.

[5] A. Mangalum, R. J. Gilliard, J. M. Hanley, A. M. Parker and R. C. Smith, *Org. Biomol. Chem.,* **2010**, *8*, 5620-5627.

[6] M. J. Plater, J. P. Sinclair, S. Aiken, T. Gelbrich and M. B., Hursthouse, *Tetrahedron,* **2004**, *60*, 6385-6394.

[7] C.-Z. Zhou, T. Liu, J.-M. Xu and Z.-K. Chen, *Macromolecules,* **2003**, *36*, 1457-1464.

[8] I. Noviandri, K. N. Brown, D. S. Fleming, P. T. Gulyas, P. A. Lay, A. F. Masters and L. Phillips, *J. Phys. Chem. B*, **1999**, *103*, 6713-6722.

[9] F. Barrière and W. E. Geiger, *J. Am. Chem. Soc.*, **2006**, *128*, 3980-3989.

[10] M. J. Frisch, G. W. Trucks, H. B. Schlegel, G. E. Scuseria, M. A. Robb, J. R. Cheeseman, G. Scalmani, V. Barone, B. Mennucci, G. A. Petersson, H. Nakatsuji, M. Caricato, X. Li, H. P. Hratchian, A. F. Izmaylov, J. Bloino, G. Zheng, J. L. Sonnenberg, M. Hada, M. Ehara, K. Toyota, R. Fukuda, J. Hasegawa, M. Ishida, T. Nakajima, Y. Honda, O. Kitao, H. Nakai, T. Vreven, J. A. Montgomery Jr., J. E. Peralta, F. Ogliaro, M. J. Bearpark, J. Heyd, E. N. Brothers, K. N. Kudin, V. N. Staroverov, R. Kobayashi, J. Normand, K. Raghavachari, A. P. Rendell, J. C. Burant, S. S. Iyengar, J. Tomasi, M. Cossi, N. Rega, N. J. Millam, M. Klene, J. E. Knox, J. B. Cross, V. Bakken, C. Adamo, J. Jaramillo, R. Gomperts, R. E. Stratmann, O. Yazyev, A. J. Austin, R. Cammi, C. Pomelli, J. W. Ochterski, R. L. Martin, K. Morokuma, V. G. Zakrzewski, G. A. Voth, P. Salvador, J. J. Dannenberg, S. Dapprich, A. D. Daniels, Ö. Farkas, J. B. Foresman, J. V. Ortiz, J. Cioslowski and D. J. Fox, Gaussian 09, (**2009**) Gaussian, Inc., Wallingford, CT, USA.

[11] T. Yanai, D. P. Tew and N. C. Handy, *Chem. Phys. Lett.*, **2004**, *393*, 51-57.

[12] J. Tomasi, B. Mennucci and R. Cammi, *Chem. Rev.*, **2005**, *105*, 2999-3093.

[13] J. E. Barnsley, S. Ø. Scottwell, A. B. S. Elliott, K. C. Gordon and J. D. Crowley, *Inorg. Chem.,* **2016**, *55*, 8184-8192.

[14] N. M. O'Boyle, A. L. Tenderholt and K. M. Langner, *J. Comput. Chem.,* **2008**, *29*, 839-845.

[15] J. C. Earles, K. C. Gordon, A. W. I. Stephenson, A. C. Partridge and D. L. Officer, *Phys. Chem. Chem. Phys.,* **2011**, *13*, 1597.

[16] G. M. Sheldrick, *SADABS: Program for Absorption Correction*. University of Goettingen: Goettingen, Germany, **1996**.

[17] L. J. Barbour, *J. Supramol. Chem.,* **2001**, *1*, 189-191.

[18] G. M. Sheldrick, *Acta Crystallogr., Sect. A: Found. Crystallogr.,* **2008**, *64*, 112-122.